Radiology Case Reports 16 (2021) 2646–2650

Available online at www.sciencedirect.com

ScienceDirect

journal homepage: www.elsevier.com/locate/radcr

Case Report

Computed tomography features of pulmonary metastases from angiosarcoma: Lessons learned from one case study ☆,☆☆

Nina M. Adzic, MD[a], *Katarina V. Obradovic, MD*[a], *Vladimir P. Urban, MD*[a], *Marija B. Mijaljevic, MD*[a], *Branka J. Radmanovic, MD*[b], *Zorica C. Milosevic, MD*[a,c,*]

[a] *Institute of Oncology and Radiology of Serbia, Department or Radiology, Belgrade, Serbia*
[b] *Institute of Oncology and Radiology of Serbia, Clinic of Surgical Oncology, Belgrade, Serbia*
[c] *School of Medicine, University of Belgrade, Belgrade, Serbia*

ARTICLE INFO

Article history:
Received 28 May 2021
Revised 14 June 2021
Accepted 16 June 2021

Keywords:
Angiosarcoma
Pulmonary Metastases
Computed Tomography

ABSTRACT

A distinctive feature of some angiosarcomas is that two or more atypical forms of pulmonary metastases may be detected concomitantly. In this case report, we present a 37-year-old man diagnosed with angiosarcoma of the neck, with extreme diversity of lung metastases on chest computed tomography (CT). We analyzed CT features of metastases and discussed possible reasons for their pleomorphism, as well as clinical implications of these findings.

© 2021 The Authors. Published by Elsevier Inc. on behalf of University of Washington. This is an open access article under the CC BY-NC-ND license (http://creativecommons.org/licenses/by-nc-nd/4.0/)

Introduction

Angiosarcoma is an aggressive malignant neoplasm of vascular or lymphatic origin, accounting for 2% of soft-tissue sarcomas, with predilection for the skin of the head and neck, while less commonly originating from the deep soft tissues. [1] The most common metastatic sites are lungs, liver, bones and lymph nodes. [2],[3] Metastatic angiosarcoma (MAS) remains an incurable disease, despite systemic therapy (anthracyclines, taxanes, tyrosine kinase inhibitors) or with a nonselective beta-blocker, propranolol, in combination with certain chemotherapy drugs. [4],[5]

The symptoms of pulmonary MAS are nonspecific (dyspnea, chest pain, cough, hemoptysis). The broad spectrum of chest CT findings includes nodules, miliary pattern, cysts, cavities, ground-glass attenuation, consolidation, tree-in-bud pattern, septal thickening, pneumothorax, hemothorax and lymph node enlargement. More than one type of lesions may be detected concomitantly. [6-12]

☆ *Competing Interest*: The authors herewith declare no conflicts of interest.
☆☆ Patient consent: This case report includes the findings in the course of clinical work and has no ethical implications.

* *Corresponding author*.
E-mail address: prof.milosevicz@ncrc.ac.rs (Z.C. Milosevic).

https://doi.org/10.1016/j.radcr.2021.06.044

1930-0433/© 2021 The Authors. Published by Elsevier Inc. on behalf of University of Washington. This is an open access article under the CC BY-NC-ND license (http://creativecommons.org/licenses/by-nc-nd/4.0/)

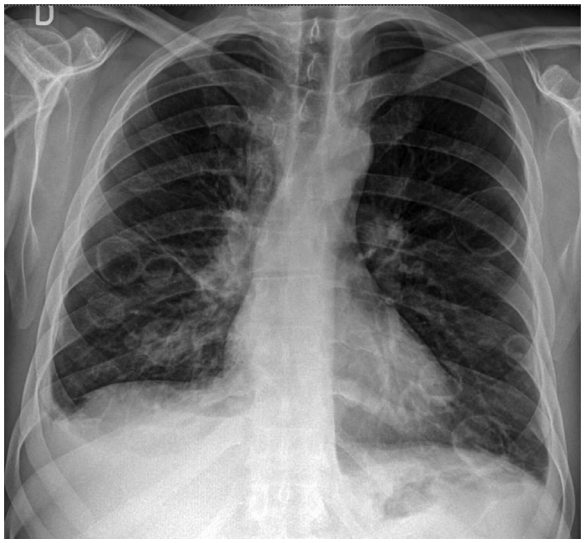

Fig. 1 – Chest radiography shows bilateral pneumatoceles in the middle and lower lung fields, measuring up to 5.0 cm, and an obtuse right costophrenic angle

Here we report a case of extreme diversity of lung metastases on chest CT in a patient with primary neck angiosarcoma.

Case report

A 37-year-old man with MAS was admitted to the Oncology institute nine days after the fourth application of doxorubicin. Pneumonia was suspected, based on dyspnea, chest pain, hemoptysis, fever (38.8°C) and chest radiograph (Fig. 1).

Four months earlier, the patient was diagnosed with cutaneous angiosarcoma of the nuchal region. Chest CT showed several pulmonary metastatic nodules, measuring 0.5–1.5 cm, and bilateral axillary lymphadenopathy. The patient underwent surgery for the primary lesion and skin grafting, followed by chemotherapy (doxorubicin).

At the admission, a residual nuchal mass and incomplete postoperative wound healing were noted. Laboratory data and blood cell count were within the normal range, except for a mildly elevated ALT, γGT, LDH serum levels, CRP (125.0 mg/L, normal≤5.0 mg/L), and erythrocyte sedimentation rate (ESR) 80. Empirical parenteral antibiotic therapy was introduced (Ceftazidime, Levofloxacin). Prior to antibiotics, bacterial cultures of blood, wound, urine and sputum were obtained, with negative results. Chest CT was performed (Fig. 2 A-J). In comparison with the initial chest CT, all nodules underwent transformation into cysts. Numerous additional bilateral cysts and cavities were noted. The size of cysts and cavities was 1.0–5.0 cm. The wall thickness of cavities was up to 0.8 cm. A few new nodules (0.8-1.5 cm) developed. All lesions were mainly subpleural, in the middle and both lower lobes. Also, ground-glass attenuation lesions, consolidations, septal thickening, bilateral pleural effusion and minimal left sided pneumothorax were detected.

The patient died two months later of progressive disease, after salvage chemotherapy (cyclophosphamide) and palliative radiotherapy for an osteolytic lesion of the iliac bone.

Discussion

Atypical metastases and mixed pattern of pulmonary MAS have been described previously. [12],[13] We reported a case of extreme diversity of lung metastases. To the best of our knowledge, there are no articles reporting the whole morphologic spectrum of pulmonary MAS concomitantly diagnosed on the same chest CT examination.

The discussion was focused on the morphology of metastases, the reasons for a wide variety of their radiologic appearances and the differential diagnosis between pneumonia and atypical metastases.

The pulmonary lesions were classified based on the Fleischner Society criteria. [14] Solid nodular lesions were defined as parenchymal nodules with soft-tissue attenuation of less than 3.0 cm in diameter. Cysts were defined as cystic areas of air density with a wall thickness of less than 0.2 cm. Ground-glass attenuation was defined as a hazy increase in lung opacity in which the bronchi and vessels remained visible. Consolidation was defined as an increased parenchymal density with obscured bronchi and vessels.

We detected solid nodules with/without perinodular ground-glass attenuation (halo sign), pure ground-glass attenuation nodules, and one solid nodule with punctate calcifications. Piciucchi *et al.* proposed a radiologic–pathologic correlation of pulmonary MAS. The solid nodules corresponded to metastatic cells growth in the vessel lumen and formation of perivascular nodules. The ground glass attenuation corresponded to alveolar hemorrhage, caused by fragility of the neovascular tissue. The authors emphasized that the halo sign is one of the most important findings for pulmonary MAS. [8] Tateishi *et al.* described nodular metastases associated with punctate calcifications as a radiologic expression of dystrophic calcifications due to hemorrhagic necrosis. Pulmonary metastases typically manifest as nodular lesions. Tateishi *et al.* reported the CT findings of pulmonary MAS in twenty-four patients, of whom 63% had nodules and 21% had cysts. [13] Yogi *et al.* confirmed this incidence (85% nodules, 58% cysts) in a group of thirty-three patients.[7]

On the contrary, the most frequent lesions in our patient were atypical metastases (cysts and cavities). We identified multiple cysts with/without air-fluid level, with solid material, halo sign and cysts with penetrating blood vessels. Solid material or fluid within the cysts indicated recent hemorrhage.[13] Yogi *et al.* first described cysts with penetrating blood vessels or bronchi as a distinctive feature of pulmonary MAS.[7] The proposed mechanisms of cystic MAS development were: excavation of solid nodules, infiltration of preexisting bullae by tumor cells, distension and disruption of alveolar walls through the ball-valve effect of the tumor, and tumor cell proliferation to form blood-filled cystic spaces. [3],[13],[15],[16] Un-

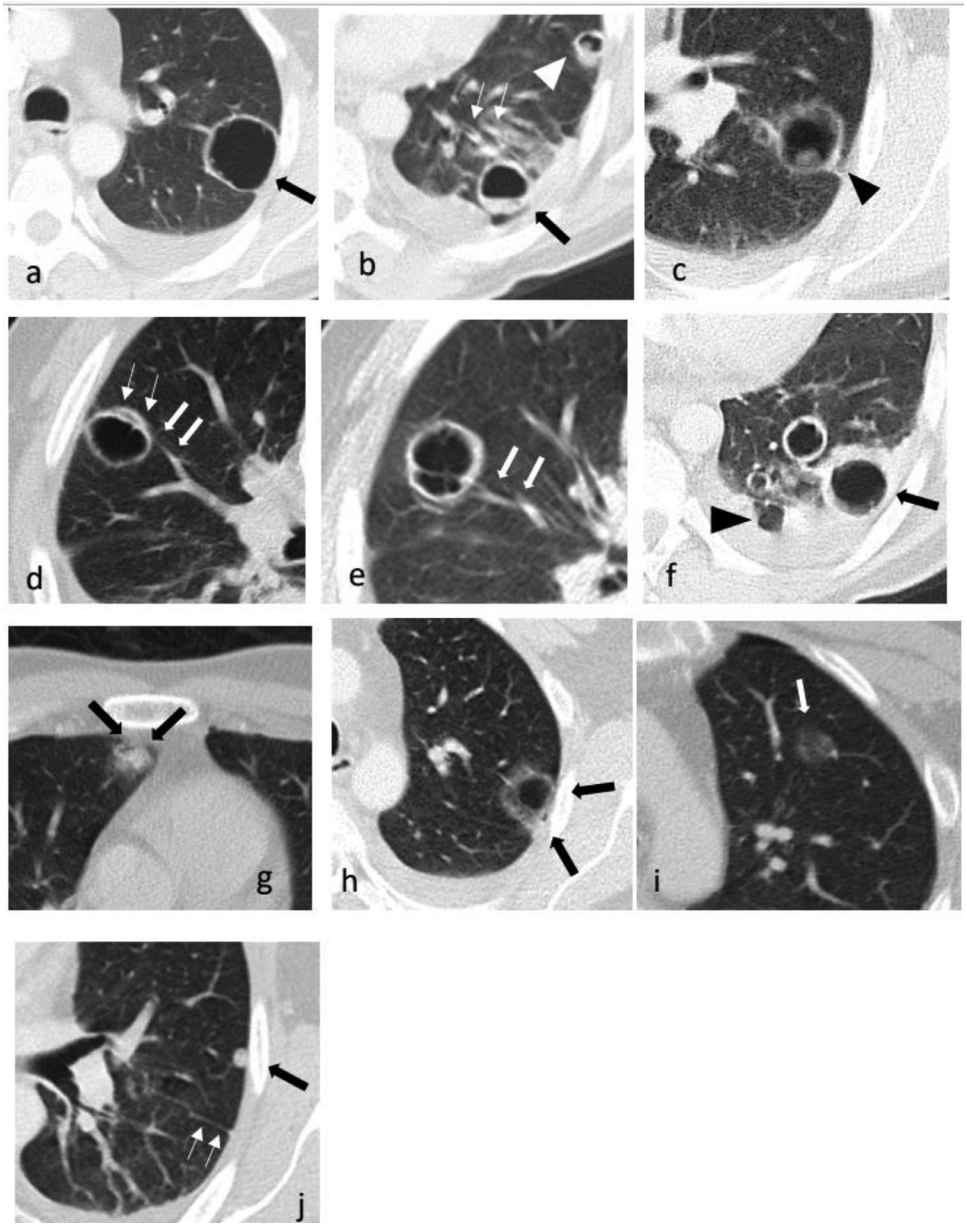

Fig. 2 – A- J. Details of contrast-enhanced transverse CT scans (lung window).
A. Subpleural cyst measuring 5.0 cm, developed from a previous subcentimeter solid nodular metastasis. Note a slightly irregular inner border of the cyst. Pleural effusion is also present.
B. Subpleural cyst with air-fluid level (arrow). Subpleural cyst with both, air-fluid level and intracystic solid, nodular lesion (arrowhead). Subsegmental ground-glass attenuation between the cysts, with focally enlarged vascular branches (small arrows).
C. Cyst with intracystic solid material (arrowhead).
D. Vessels (arrows) penetrating the cyst, mimicking double contour of the cyst wall (small arrows).
E. Vessels (arrows) penetrating the cyst, simulating multilocular cyst.
F. Cavity (arrow) with irregular wall, several cysts and pleural effusion. The arrowhead indicates the round area of air density in the subpleural, subsegmental consolidation and ground-glass attenuation.
G-I. Three different types of ground-glass attenuation: g – halo sign of 0.5 cm around a nodular lesion measuring 1.2 x 1.0 cm (two arrows), with internal punctate calcifications; h – halo sign around a cyst (two arrows); i – pure nodular ground-glass attenuation (one arrow).
J. Newly-formed solid nodule measuring 0.8 cm (arrow) and septal thickening (small arrows), suggesting lymphatic spread of tumor cells

like cysts, cavities had a thick, irregular wall (more than 0.4 cm). Cysts and cavities may represent two different stages of the same pathologic process (necrosis of initial solid mass). Rupture of subpleural cysts or cavities may cause pneumothorax or hemothorax, [8],[10],[13],[16] which was noted in our patient.

Ground-glass attenuations, as a different manifestation of pulmonary hemorrhage of MAS, [8] in our patient was represented by subsegmental areas, with/without focally enlarged vascular branches, pure ground-glass attenuation nodules, and halo sign around cysts and cavities. Similar to Aversa *et al.*, we found multiple subsegmental consolidations without air bronchogram. The formative mechanism can be the enlargement of solid metastases with associated organizing pneumonia. [8],[17]

We proposed several explanations for the peculiar CT findings in our patient. Among them, the most significant were the patient-related factors. He was a non-responder to the combined therapy, with a rapidly progressive disease and lethal outcome six months after the diagnosis. Consecutively, CT findings depicted the advanced phase of pulmonary MAS. Cheng *et al.* also described cystic metastases of pulmonary MAS that developed and enlarged within a few months. [18] Other reasons can be the different designs of case reports and series, i.e., inclusion criteria for morphology of the lesions, and different CT technique.

In our case, the first diagnostic hypothesis was pneumonia, based on the clinical symptoms, high CRP levels and ESR, and chest radiographic findings of cystic lesions – pneumatoceles. They can be seen in pulmonary infections caused by *Staphylococcus aureus, Pneumocystis jirovecii, Escherichia coli* and *Streptococcus pneumoniae*, as a consequence of airway obstruction and ball-valve mechanism. Solid nodules with halo-sign (perinodular hemorrhage) can be found in angioinvasive aspergillosis in immunocompromised patients with severe neutropenia. [19] Nevertheless, our patient had a normal white blood cell count. The blood, urine and sputum cultures were negative. The chest CT findings were highly suggestive of pulmonary MAS, particularly the halo-sign around nodules and cysts and vessels penetrating the cysts, as well as transformation of solid metastatic nodules into cysts within four months. Invasive diagnostic procedures may cause massive pulmonary hemorrhage, due to hypervascularity of MAS. [20] Chest CT, as a non-invasive imaging modality, represented a significant tool for the correct and prompt diagnosis of pulmonary metastases.

Our patient was diagnosed prior to the Coronavirus disease 2019 (COVID-19) pandemic. However, it is worth mentioning that some chest CT findings of pulmonary MAS overlap with COVID-19. The diffuse vascular tree-in-bud pattern was noted in both diseases, due to neoplastic trombotic microangiopathy of MAS, and microthrombosis with endothelial damage directly caused by the coronavirus in the case of COVID-19.[8],[21] The focal vessel enlargement within ground-glass opacities was described as the early CT manifestation of COVID-19 pneumonia, while the cavitation, pleural effusion and lymphadenopathy were rarely reported.[22],[23]

Conclusion

We presented an unusual finding of the whole morphologic spectrum of predominantly atypical pulmonary metastases, diagnosed on the same chest CT examination of a patient with neck angiosarcoma. Taking into account the ambiguous findings of chest radiography, clinical and laboratory data, the CT features were crucial for the final diagnosis of MAS progression.

REFERENCES

[1] Enzinger FM, Weiss SW. Soft tissue sarcoma. St. Louis: Mosby; 2001. p. 917–54.
[2] Young RJ, Brown NJ, Reed MW, Hughes D, Woll PJ. Angiosarcoma. Lancet Oncol 2010;11:983–91.
[3] Wang H, Shi J, Liu H, Chen Y, Wang Y, Wang W, et al. Clinical and diagnostic features of angiosarcoma with pulmonary metastases: a retrospective observational study. Medicine (Baltimore) 2017;96:e8033.
[4] Florou V, Wilky BA. Current and future directions for angiosarcoma therapy. Curr Treat Options Oncol 2018;19:14.
[5] Bi S, Chen S, Wu B, Cen Y, Chen J. The effectiveness of different treatment modalities of cutaneous angiosarcoma: results from meta-analysis and observational data from SEER database. Front Oncol 2021;25:627113.
[6] Adem C, Aubry MC, Tazelaar HD, Myers JL. Metastatic angiosarcoma masquerading as diffuse pulmonary hemorrhage: clinicopathologic analysis of 7 new patients. Arch Pathol Lab Med 2001;125:1562–5.
[7] Yogi A, Miyara T, Ogawa K, Iraha S, Matori S, Haranaga S, et al. Pulmonary metastases from angiosarcoma: a spectrum of CT findings. Acta Radiol 2016;57:41–6.
[8] Piciucchi S, Dubini A, Tomassetti S, Sanna S, Ravaglia C, Carloni A, et al. Angiosarcoma in the chest: radiologic pathologic correlation: case report. Medicine (Baltimore) 2016;95:e5348.
[9] Ajayi AA, Commins SV, Clarke DE. Metastatic angiosarcoma of the scalp presenting with cystic lung lesions: a case report and review of cystic lung diseases. Perm J 2018;22:17–168.
[10] Jimenez D, Antaki J, Kamangar N. Metastatic pulmonary angiosarcoma presenting with bilateral secondary spontaneous pneumothoraces. J Intensive Care Med 2017;32:292–6.
[11] Andersen KF, Albrecht-Beste E, Berthelsen AK, Loft A. Angiosarcoma of the scalp: metastatic pulmonary cystic lesions initially misinterpreted as benign findings on 18F-FDG PET/CT. Diagnostics (Basel). 2015;6:1.
[12] Seo JB, Im JG, Goo JM, Chung MJ, Kim MY. Atypical pulmonary metastases: spectrum of radiologic findings. Radiographics 2001;21:403–17.
[13] Tateishi U, Hasegawa T, Kusumoto M, Yamazaki N, Iinuma G, Muramatsu Y, et al. Metastatic angiosarcoma of the lung: spectrum of CT findings. AJR Am J Roentgenol 2003;180:1671–4.
[14] Hansell DM, Bankier AA, MacMahon H, McLoud TC, Müller NL, Remy J. Fleischner society: glossary of terms for thoracic imaging. Radiology 2008;246:697–722.
[15] Aryal S, Chu C, Morehead RS. An 83-year-old gentleman with bilateral spontaneous pneumothoraces and multiple cysts. Chest 2011;139:1536–9.

[16] Bocklage T, Leslie K, Yousem S, Colby T. Extracutaneous angiosarcomas metastatic to the lungs: clinical and pathologic features of twenty-one cases. Mod Pathol 2001;14:1216–25.
[17] Aversa M, Bhinder S, Tanguay J, Thenganatt J. A rare cause of hemoptysis. Respir Med Case Rep 2014;13:48–50.
[18] Cheng YS, Chen TM, Tsai WC, Huang TW. Pulmonary metastatic angiosarcoma from scalp with fatal complication: a case report. Int J Surg Case Rep 2017;34:36–9.
[19] Beigelman-Aubry C, Godet C, Caumes E. Lung infections: the radiologist's perspective. Diagnostic and Interventional Imaging 2012;93:431–40.
[20] Adem C, Aubry MC, Tazelaar HD, Myers JL. Metastatic angiosarcoma masquerading as diffuse pulmonary hemorrhage: clinicopathologic analysis of 7 new patients. Arch Pathol Lab Med 2001;125:1562–5.
[21] Levi M, Iba T. COVID-19 coagulopathy: is it disseminated intravascular coagulation? Intern Emerg Med 2021;16:309–12.
[22] Han R, Huang L, Jiang H, Dong J, Peng H, Zhang D. Early clinical and CT manifestations of coronavirus disease 2019 (COVID-19) pneumonia. AJR Am J Roentgenol 2020;215:338–43.
[23] Duzgun SA, Durhan G, Demirkazik FB, Akpinar MG, Ariyurek OM. COVID-19 pneumonia: the great radiological mimicker. Insights Imaging 2020;11:118.